Proceedings of the International Conference on Heat Exchanger Fouling and Cleaning - 2024 (Peer-reviewed)
April 21–26, 2024, Lisbon, Portugal; Editors: H.U. Zettler and E.M. Ishiyama

INFLUENCE OF SURFACE TEXTURE ON THE CLEANABILITY OF 3D-PRINTED STAINLESS-STEEL COMPONENTS

T. Hanisch[1], S. Stelzer[2], V. Eisenrauch[1]*, N. Milaev[2], J. Thielsch[2], S. Jacob[1], E. Fuchs[1], M. Mauermann[1]
[1] Fraunhofer Institute for Process Engineering and Packaging IVV, Division Processing Technology, Heidelberger Str. 20, 01189 Dresden, Germany
vincent.eisenrauch@ivv-dd.fraunhofer.de (corresponding author)
[2] Fraunhofer Institute for Machine Tools and Forming Technology IWU, Dresden, Germany

ABSTRACT

Metallic 3D printing holds immense potential, yet its application in the food and pharmaceutical sectors is hampered by surface roughness that exceeds hygienic standards. This study investigates the effect of post-processing methods and macrostructures on surface properties, soiling behavior and cleanability of 3D-printed components for hygienic purposes. All investigated post-processing methods effectively reduce surface roughness. Soiling behavior analysis shows reduced initial surface soil coverage, particularly with lower average surface roughness and the introduction of protrusions. Cleaning tests demonstrate significantly reduced macroscopic cleaning time and microbial contamination, particularly with abrasive flow machining and protrusion incorporation. However, residual microbial contamination remains higher in 3D-printed components than in conventionally manufactured pipes. Combining post-processing with macro-structuring further improves microbial cleanability, reaching levels comparable to conventionally manufactured pipes. These results highlight the efficacy of post-processing methods and macrostructure incorporation in enhancing cleaning efficiency in 3D-printed components for hygienic applications.

INTRODUCTION

The widespread adoption of additive manufacturing, commonly known as 3D printing, is driven by its immense potential in industries as diverse as aerospace, automotive, biomedical and consumer goods [1]–[4]. This technology offers benefits such as adaptability, design freedom, optimal material utilization and rapid prototyping [5].

In the field of heat exchanger design and development, additive manufacturing has opened new avenues [6]. The economic sustainability of heat exchangers depends on efficient heat transfer, which requires systematic modifications on internal flow through methods such as inserts, fins or corrugated surfaces [7]. The advanced capabilities of additive manufacturing technologies enable engineers to create geometric designs with both internal and external complexities, enhancing heat transfer efficiency while minimizing pressure drop [8].

Special considerations arise in the context of heat exchangers utilized in food and pharmaceutical production. The stringent demands of these industries on material properties, particularly for surfaces in contact with the product, make the use of stainless steel in process line components a logical consequence due to its advantageous mechanical properties and resistance to corrosion and oxidation [9]. The Laser Powder Bed Fusion (LPBF) manufacturing process is emerging as a promising technology for additively manufacturing stainless steel. However, the inherent nature of the LPBF process results in components with high surface roughness, contradicting hygienic design principles that advocate for a low roughness of $R_a < 0.8$ µm [10]. Consequently, additively manufactured components face limitations in the food and pharmaceutical industries due to increased fouling and cleaning challenges, rendering them inferior to conventionally manufactured counterparts [11].

There are two possible strategies to compensate for the negative effect on cleanability caused by the inadequate surface microstructure. The first is to finish the surfaces to reduce the roughness. Suitable post-processing methods for internal channels are mechanical finishing processes such as abrasive flow machining (AFM) or electrochemical processes such as Hirtisation and electropolishing [12].

The second possible strategy is to modify the macrostructure of the surface to improve the convective transport processes near the surface [13], [14]. While extensive research has focused on the heat transfer augmentation of macrostructures, limited literature addresses their impact on cleaning

ISBN: 978-0-9984188-3-4; Published online www.heatexchanger-fouling.com

processes. Hanisch et al. [15] demonstrated that surface modifications can improve the cleanability of a 3D-printed component, with a reduction in microbial contamination of over 90 % for a dimpled surface. Another study also demonstrated the positive effect on cleanability for teardrop-shaped protrusions [16].

In this paper, we investigate the influence of common post-processing methods and macro-structuring on the surface texture of pipes manufactured with LPBF. Furthermore, the influence on soiling behavior and macroscopic and microbial cleanability is studied. The effect of post-processing methods and surface macro-structuring are compared in order to identify effective strategies for improving the cleanability in LPBF-manufactured pipes. Finally, the combination of both strategies is investigated and compared to a conventionally manufactured pipe.

MATERIALS AND METHODS

Additive manufacturing and post processing

The Laser Powder Bed Fusion manufacturing process was used to produce the standardized internal pipe geometry made of 1.4404 (stainless steel). In this process (Fig. 1), powder layers are applied by a coater and the powder particles per layer are melted by a laser at the position specified by the CAD file.

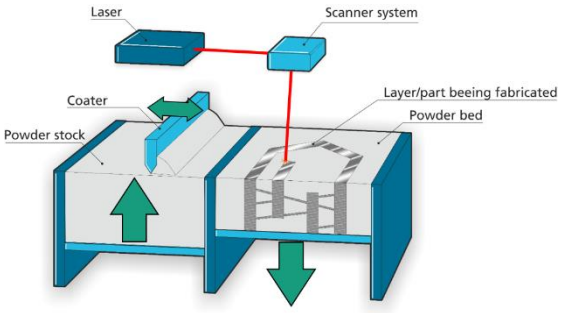

Fig. 1. Schematic representation of the Laser Powder Bed Fusion process for metal

The used laser-parameters of the Trumpf TruPrint1000 for 1.4404 stainless steel are shown in Table 1. The manufactured inner pipe geometry (Fig. 2), with an inner diameter of 25 mm and tri-clamp connections for integration into the cleaning test stand, is designed to be separable and was manufactured with and without a surface macro-structuring. The advantages of the selected teardrop-shaped protrusion structure are described in detail in [16].

Table 1: Standard parameters of the TruPrint1000 for 1.4404

Standard parameters	**Values**
Layer thickness	20 µm
Beam diameter	30 µm
Scanning speed	700 mm/s
Laser power	120 W

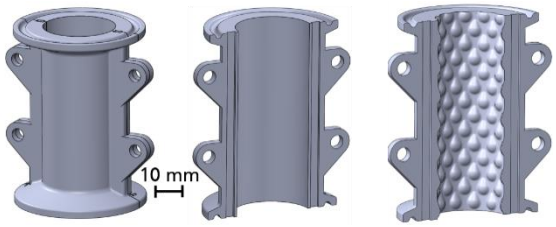

Fig. 2. Manufactured separable geometry without structuring (center) and with structuring (right)

Following the production and removal of the components from the building panel, the unstructured components were post-processed using suitable finishing processes for internal channels. The process was repeated with the most effective post-processing method for the structured geometry.

With AFM, Hirtisation and electropolishing, the most suitable post-processing methods to reduce the roughness were used for the produced internal structures. While AFM is a mechanical finishing process in which a paste containing abrasive particles is forced through internal channels under high pressure [12], the other two methods mentioned are electrochemical finishing processes. Electro-polishing is an established finishing process in which metal rods are inserted as cathodes into the internal areas to be post-processed. Within the Hirtisation process, which is primarily used for 3D-printed metal components, only electrochemical liquids are used, which are pumped through the areas which need to be post-processed [17].

Surface texture and 3D scans

The optical 3D profilometer VR-5000 from Keyence, which uses the light section method, was used to evaluate the surface texture. Based on the applicable surface properties for the manufactured metal components, the characteristic values according to the standard shown in Table 2 were applied.

Table 2: Keyence magnification and settings according to DIN EN ISO 21920-3

Specified parameter	**Setting**
Keyence Magnification	80 x
Evaluation length	12.5 mm
Coherence length λ_C	2.5 mm
Cut-off wavelength λ_S	8 µm

Roughness measurements were performed on all unstructured surfaces. As there is no suitable

ISBN: 978-0-9984188-3-4; Published online www.heatexchanger-fouling.com

standardized measuring section on structured surfaces, the values for the unstructured section can be assumed. In addition, the same equipment was used to take 3D surface images of all samples as well as profile images of the structured components. Since the partially glossy surfaces were unsuitable for optical evaluation due to post-processing, an anti-reflective spray (MR 2000) suitable for optical measuring equipment was used where necessary.

Soiling procedure

Sour milk served as a food-based soil for cleaning tests, mirroring the EHEDG cleaning test for assessing the in-place cleanability of food processing equipment [18]. Its preparation involved mixing 1 liter of low-fat milk with 0.1 grams of a mesophilic culture (Danisco Choozit MM 100 LYO 25 DCU) and subsequent incubation at $T = 30$ °C for 18 hours. After homogenization, the material was applied to the test sections. These pipe sections were filled, sealed, mechanically stressed for 60 seconds with a vortex mixer, and then stored upright to allow soil drainage. After final drying at $T = 23$ °C and 50 % relative humidity for 24 hours, an individual, inhomogeneous distribution of dried soil was obtained for each post-processed test section. The initial surface soil coverage $m''_{s,0}$, was gauged through the differential weighing of the test sections before soiling and after the drying process.

Cleaning experiments

The cleaning experiments, extensively described in [15], were based on the EHEDG cleanability test [18], a well-established certification test for hygienic design and easy cleanability of equipment. The parameters were adjusted to facilitate a quantitative comparison.

For the cleaning tests, the test sections were placed in a test rig as shown in Fig. 3. A centrifugal pump circulated a mild, alkaline cleaning fluid (following EHEDG Guideline 2 [18]) at $T = 63$ °C. Cleaning procedures differed depending on whether macroscopic or microbial cleaning behavior was investigated. A summary of the parameters for cleaning is given in Table 3.

For macroscopic cleaning behavior, a UV-optical method was employed to observe the transient removal of soil with high spatial resolution. One printed half of each metal pipe was connected to an upper side made of acrylic glass. This facilitated exciting the soil layer with UVA light (365 nm), and images were recorded at a rate of 1 frame per second using an industrial camera. The local fluorescence intensity correlates with soil layer thickness [19] and was used for observation of the cleaning progress. In preliminary tests, it was found that dried sour milk is comparatively easy to remove. Therefore, the mean velocity in the test sections was reduced from $u = 1{,}5\ \mathrm{m/s}$ in the EHEDG test to $u = 0{,}34\ \mathrm{m/s}$ in order to be able to detect relevant differences at the given frame rate. Macroscopic cleaning experiments were replicated four times for statistical confidence.

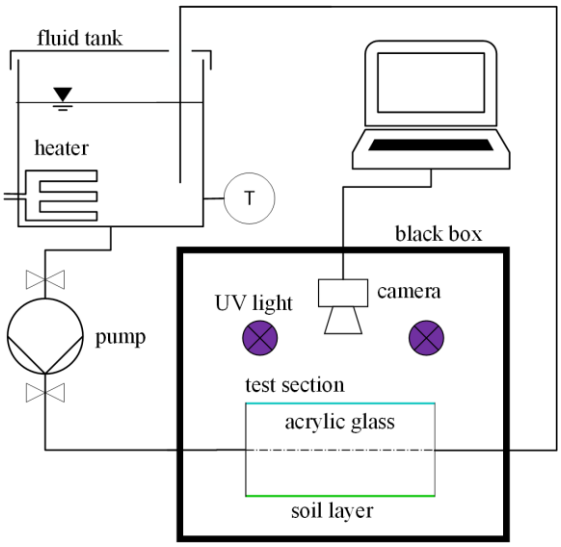

Fig. 3. Schematic drawing of the cleaning test rig.

To evaluate microbial cleaning behavior, a spore suspension of *Geobacillus stearothermophilus* was added to the soil resulting in a contamination level characterized by a concentration of 10^5 colony forming units (CFU) per milliliter. These spores remained on the pipe surface, even after the visible soil film had disappeared under UV light and were more difficult to remove. The recommended average velocity of $u = 1{,}5\ \mathrm{m/s}$ from the EHEDG test was applied, and the microbial cleaning tests were replicated six times to ensure statistical certainty.

Table 3. Parameters used for the investigation of macroscopic and microbial cleaning.

	Macroscopic cleaning	**Microbial cleaning**
Pre-rinsing time with demineralized water at room temperature in min	-	1
Cleaning time in min	2.5	18
Final rinsing time with demineralized water at room temperature in min	-	1
Average flow velocity in m/s	0,34	1,5

Detection of residual microbial contamination was accomplished by subsequent filling of the test sections with Shapton and Hinds (SHA) agar. After incubation at $T = 58$ °C for 24 hours, areas with

ISBN: 978-0-9984188-3-4; Published online www.heatexchanger-fouling.com

remaining microbes showed a yellow discoloration. Quantitative evaluation involved dividing the outer layer of agar into 4 parts and analyzing the yellow discolored area using transmitted light, see Fig. 4.

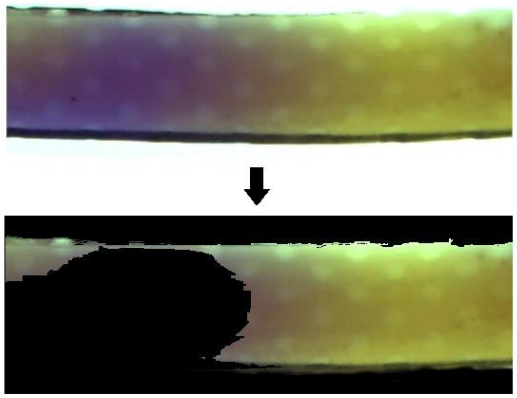

Fig. 4. Illustration of the procedure for quantitative evaluation of residual microbial contamination by color change in the agar. Reprinted from [16] with permission from Elsevier.

RESULTS AND DISCUSSION

Surface texture

Following the production of the unstructured components, the roughness measurement was carried out on the as-built and post-processed surfaces. (Table 4). A conventionally manufactured reference pipe with a 2B surface finish according to DIN EN 10088-2 ($R_a = 0.5$ µm) serves as the standard of comparison. It is referred to below as the "reference pipe". The aim is either to achieve this standard or at least to demonstrate comparable cleaning results.

Table 4: Average roughness values of the as-built and post-processed components:

Part type	**Average roughness R_a**
Reference pipe	0.5 µm
As built	4.3 µm
Electropolishing	2.4 µm
Hirtisation	1.0 µm
AFM	0.7 µm

As expected, the roughness of the non-processed samples ("as built") is highest at 4.3 µm. The insufficient roughness values are process-related in the LPBF process for metal and must be post-processed for functional use in the food and pharmaceutical industries. The studied post-processing methods lead to an improved surface quality but reveal a large variation in the roughness values achieved. While electrochemical post-processing methods generally achieve very good, geometry-preserving post-processing results, their application to internal geometries is only possible to a limited extent. On the one hand, this is due to the process-related need to integrate the cathode within the inner channel to be machined. On the other hand, the necessary electrolytes must be flushed through the pipe geometry to counteract the gas formation that occurs during the electropolishing process. These two factors may have led to poorer material removal. In comparison, better surface values could be achieved by Hirtisation, which does not require an internal cathode. AFM, as a mechanical post-processing method, achieved the best roughness values at 0.7 µm. However, the direct application of mechanical force, with up to 100 bar grinding pressure, produces scratch marks that are typical for the AFM process. This results in topographical anisotropy which may affect the wetting and cleanability of the surface [20]. Fig. 5 shows the manufactured as built components in comparison to the AFM post-processing with the adjacent enlarged micrograph of the surface.

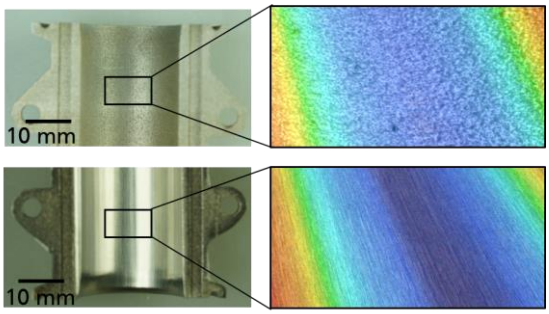

Fig. 5. As built component (top left), microscope image (top right) and AFM post-processed component with typical grinding marks (bottom left), microscope image (bottom right).

Since the AFM process provides the lowest surface roughness, this post-processing method was used for the structured component. Fig. 6 shows the material removal of the profile height of the structured component by AFM compared to the as built component. The material removal led to a reduction in the structure height of approximately 0.15 mm, while the general profile was retained.

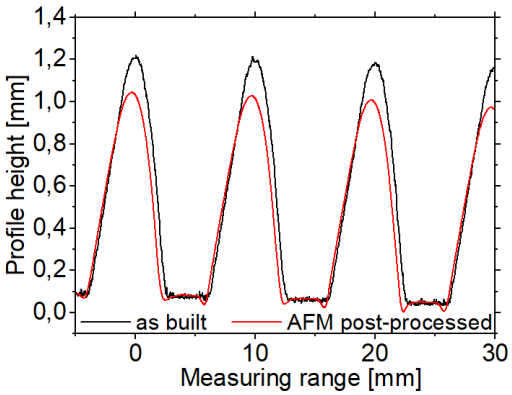

Fig. 6. Material removal of the structured part by AFM compared to the as built component.

ISBN: 978-0-9984188-3-4; Published online www.heatexchanger-fouling.com

Soiling behavior

The initial focus lies on presenting the impact of surface texture on soiling behavior. As each pipe has a slightly different surface area, the measured soil mass was normalized with the surface area. This variable, referred to as surface soil coverage, represents the fouling behavior under the specific conditions of our soiling procedure.

Fig. 7 illustrates the dependence of mean initial surface soil coverage on the surface texture. All post-processing methods applied demonstrate a reduction in initial surface soil coverage compared to the as-built component. This reduction is more pronounced with lower average surface roughness.

Adding protrusions onto the surface also hinders the build-up of soil in comparison to the component as built. The investigated teardrop-shaped protrusion leads to a 25 % reduction in surface soil coverage.

A one-way analysis of variance (ANOVA) was conducted to compare the effect of the surface texture on initial surface soil coverage. There was a statistically significant difference in mean initial surface soil coverage at the $p < 0.05$ level between at least two groups [$F(4, 13) = 9.13$, $p = 0.0001$].

Post-hoc comparisons using Tukey's range test [21] indicated that the mean value of initial surface soil coverage of the as-built component was significantly higher than that of the component treated with Hirtisation ($p = 0.0085$, 95 % confidence interval (C.I.) = [2.51, 18.45]) and that of the component treated with AFM ($p = 0.00045$, 95 % C.I. = [6.83, 22.77]). There was no statistically significant difference between the other groups.

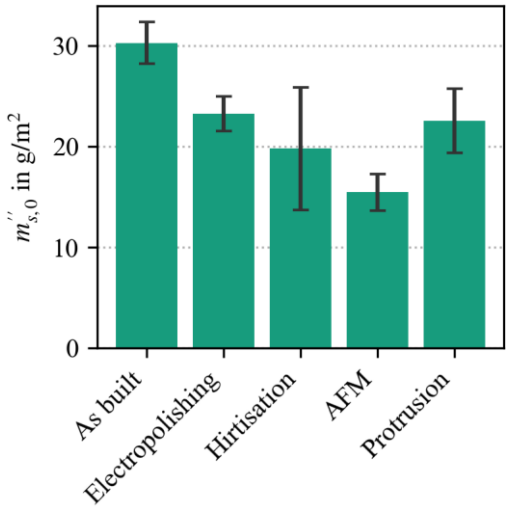

Fig. 7. Initial surface soil coverage depending on the surface macro- and microstructure. Error bars are representing standard deviations.

Cleaning results

Macroscopic cleaning

The time course of the normalized surface soil coverage is used to analyze the macroscopic cleaning process, see Fig. 8. For this purpose, the surface soil coverage of each component under investigation was normalized with the value at the beginning of the cleaning test. This allows for a direct comparison of the cleaning rate independent of the initial surface soil coverage.

The first observation is that all components are macroscopically clean after a cleaning time of 150 seconds, i.e., no more residues can be detected using the optical method. Furthermore, the results show that both the use of post-processing methods and the application of macrostructures lead to an improvement in cleanability.

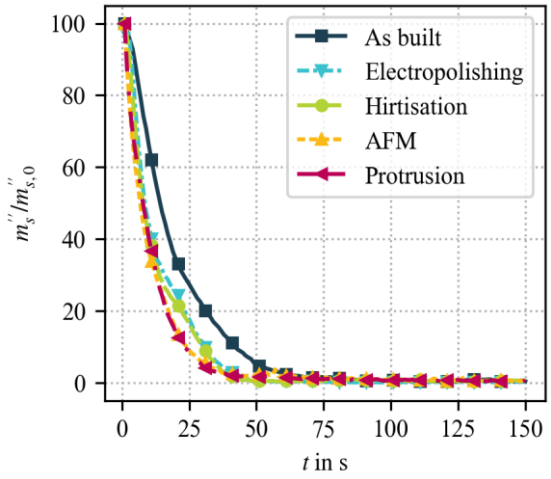

Fig. 8. Development of normalized surface soil coverage over time depending on the surface texture

The cleaning time t_{95}. is used for a quantitative comparison of the studied surface modifications. It is defined as the time after which 95 % of the initial soil mass has been removed and is shown in Fig. 9.

The electrochemical post-processing methods electropolishing and Hirtisation lead to a decrease of mean cleaning time from 51 to 36 and 35 seconds respectively. Post-processing with AFM as well as adding protrusions on the surface have an even greater effect. They reduce the mean cleaning time by more than 40 % to 28 and 29 seconds respectively.

ISBN: 978-0-9984188-3-4; Published online www.heatexchanger-fouling.com

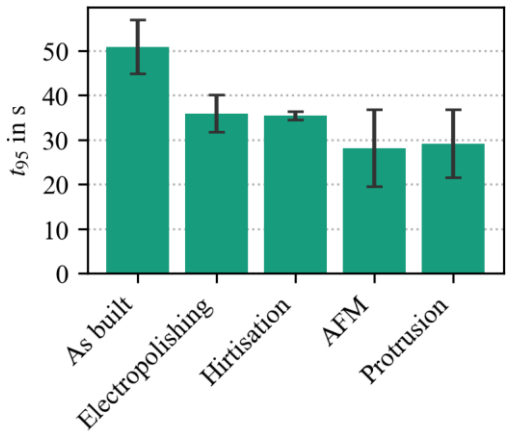

Fig. 9. Mean cleaning time depending on the surface texture.

To assess the impact of surface texture on mean cleaning time, a one-way ANOVA was executed. The findings indicated a statistically significant effect on mean cleaning time for the five components investigated [F(4, 13) = 8.15, p = 0.0016].

Post-hoc examinations utilizing Tukey's test showed significant differences in mean cleaning time at the p<0.05 level. Notably, the as-built component exhibited a significant difference in mean cleaning time compared to components treated with Hirtisation (p = 0.03, 95 % C.I. = [1.26, 29.63]) and AFM (p = 0.002, 95 % C.I. = [8.59, 36.96]), as well as the component featuring protrusions (p = 0.003, 95 % C.I. = [7.54, 35.91]). , these results indicate that almost all of the studied modifications of the pipe's surface texture lead to a significant reduction in cleaning time at the macroscopic level.

Microbial cleaning

In the food industry, in addition to macroscopic cleanliness, microbial cleanliness must also be guaranteed. This was assessed by sampling the pipes with SHA agar after the cleaning experiments, as described above.

Fig. 10 displays the mean residual microbial contamination on the surface of the investigated test sections after the microbial cleaning tests. For a better overall evaluation, these values were also compared with the results of the conventionally manufactured reference pipe.

The results show that microbial contamination was detected on 77 % of the surface of the as-built component after the cleaning tests. This is attributed to the high surface roughness of the wall, making it difficult, if not virtually impossible, to remove the microbial contamination. Bobe [22] showed that the cleanability of the contaminated sour milk used here significantly deteriorates at a roughness (R_a) greater than 0.9 µm. At R_a = 4.3 µm, the surface roughness of the as-built component falls far below the recommended standard.

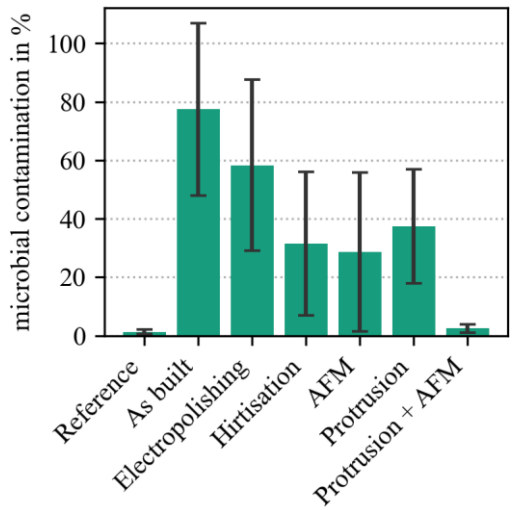

Fig. 10. Mean residual microbial contamination after the cleaning experiments depending on the surface texture.

All post-processing methods resulted in an enhancement of microbial cleanliness. Among the methods examined, AFM demonstrated the most promising results. Pipes that underwent post-processing using this method exhibited a mean residual microbial contamination of less than 30 %. According to Bobe's research [22], below R_a = 0.9 µm, there is scarcely any difference in microbial cleanability, which explains the nearly identical results of Hirtisation and AFM. Apart from post-processing the surface, the implementation of the protrusion structure contributed to a substantial reduction in residual microbial contamination, reducing it to 37 %.

A one-way ANOVA confirmed the statistical significance of the observed effects on microbial contamination [F(6, 34) = 8.70, p = 9.1e-6]. Post-hoc examinations using Tukey's test showed significant differences between the as-built component and the components treated with Hirtisation (p = 0.02, 95 % C.I. = [5.24, 86.64]) and AFM (p = 0.01, 95 % C.I. = [8.01, 89.41]).

Nevertheless, the cleanliness of all investigated 3D-printed test sections with surface modification was far away from the result of the conventionally manufactured reference pipe, which had almost no residual microbial contamination. This is remarkable because the test section, which was subjected to AFM after manufacturing, only had a slightly higher average roughness of R_a = 0.7 µm. This value is even lower than the recommended value of R_a = 0.8 µm by the EHEDG in its Hygienic Design Principles [10]. However, the R_a value is only of limited significance as it is primarily the surface topography that determines cleanability. As shown in Fig. 5, the AFM process leads to small micro-grooves in the surface caused by the abrasive

ISBN: 978-0-9984188-3-4; Published online www.heatexchanger-fouling.com

particles within the paste. The resulting surface topography may adversely affect cleanability.

A substantial improvement in microbial cleanability was achieved by combining post-processing using AFM and macro-structuring with protrusions, as shown by the rightmost bar in Fig. 10. By combing these measures, the residual microbial contamination was reduced to 2.5 % and is of the same order of magnitude as for the reference pipe.

CONCLUSION

The study's findings bear significant implications for the application of 3D printing in the food and pharmaceutical industry. The investigated post-processing methods like AFM and Hirtisation, showcase a substantial improvement in both surface roughness and soiling behavior of 3D-printed pipe components compared to the non-processed part. The introduction of teardrop-shaped protrusions on the surface also leads to a significant improvement in the soiling behavior.

The reduced initial surface soil coverage and enhanced cleanability suggest that these modified components are better suited for food and pharmaceutical processing environments where hygiene is paramount. However, challenges persist, notably in microbial cleanliness. Despite advancements, residual microbial contamination remains higher in all 3D-printed components than in conventionally manufactured pipes.

A potential way forward is the combination of a cleaning-promoting surface structure and post-processing. In our study, the combination of AFM and macro-structuring with protrusions, for example, achieved a microbial cleanability comparable to that of the conventionally manufactured reference pipe.

To further optimize 3D-printed components for the food and pharmaceutical industry, a multifaceted approach is recommended. First, the evaluation and optimization of suitable post-processing methods to further decrease surface roughness and microbial contamination is crucial. Second, the targeted optimization of the surface macrostructure using flow simulation is to be continued. Additionally, additive manufacturing offers the possibility of applying innovative surface coatings that are firmly bonded to the base material and could mitigate contamination concerns.

Our future research will focus in particular on improving electrochemical post-processing methods for internal geometries as well as on the simulation-based optimization of the surface macrostructure to increase cleaning efficiency. As shown, the surface quality of the electropolished components was the worst compared to the other post-processing methods. A significant improvement could be achieved by 3D printing the cathode required for the process. The patented method [23] is to be investigated in the follow-up project. Furthermore, simulation approaches are being developed for the contour optimization of complex curved geometries to improve the cleanability of industrially relevant components. In order to decide whether conventional or additive manufacturing is more suitable for practical industrial applications, a comprehensive consideration of energy and resource consumption over the entire life cycle of the component should also be carried out.

ACKNOWLEDGMENTS

The IGF project (20790 BR) is supported by the Research Association of the Industrial Association for Food Technology and Packaging (IVLV e.V.) and is funded by the Federal Ministry for Economic Affairs and Climate Action via the AiF as part of the program for the promotion of industrial community research (IGF) based on a decision of the German Bundestag.

NOMENCLATURE

m_s''	surface soil coverage	g/m^2
$R_{a\square}$	arithmetic mean roughness height	µm
T	temperature	°C
t_{95}	time after which 95 % of the initial soil mass is removed	s
u	mean velocity	m/s

Greek symbols

λ_C	Coherence length of the light	mm
λ_S	Cut-off wavelength of the scattering	mm

Subscript

0	initial

Acronyms

AFM	abrasive flow machining
ANOVA	analysis of variance
LPBF	Laser Powder Bed Fusion
SHA	Shapton and Hinds

REFERENCES

[1] B. Blakey-Milner, P. Gradl, G. Snedden, M. Brooks, J. Pitot, E. Lopez, M. Leary, F. Berto, and A. du Plessis, Metal additive manufacturing in aerospace: A review, *Materials & Design*, vol. 209, p. 110008, 2021.

[2] Z. Mehdiyev and C. Felho, Metal Additive Manufacturing in Automotive Industry: A Review of Applications, Advantages, and Limitations, *Materials Science Forum*, vol. 1103, pp. 49–62, 2023.

[3] Y. Zhai, H. Zhang, J. Wang, and D. Zhao, Research progress of metal-based additive manufacturing in medical implants, *REVIEWS ON ADVANCED MATERIALS SCIENCE*, vol. 62, no. 1, 2023.

ISBN: 978-0-9984188-3-4; Published online www.heatexchanger-fouling.com

[4] S. Rouf, A. Malik, N. Singh, A. Raina, N. Naveed, M. I. H. Siddiqui, and M. I. U. Haq, Additive manufacturing technologies: Industrial and medical applications, *Sustainable Operations and Computers*, vol. 3, pp. 258–274, 2022.
[5] K. Kanishka and B. Acherjee, Revolutionizing manufacturing: A comprehensive overview of additive manufacturing processes, materials, developments, and challenges, *Journal of Manufacturing Processes*, vol. 107, pp. 574–619, 2023.
[6] I. Kaur and P. Singh, State-of-the-art in heat exchanger additive manufacturing, *International Journal of Heat and Mass Transfer*, vol. 178, p. 121600, 2021.
[7] S. S. Mousavi Ajarostaghi, M. Zaboli, H. Javadi, B. Badenes, and J. F. Urchueguia, A Review of Recent Passive Heat Transfer Enhancement Methods, *Energies*, vol. 15, no. 3, Art. no. 3, 2022.
[8] D. Jafari and W. W. Wits, The utilization of selective laser melting technology on heat transfer devices for thermal energy conversion applications: A review, *Renewable and Sustainable Energy Reviews*, vol. 91, pp. 420–442, 2018.
[9] F. Andreatta, A. Lanzutti, E. Vaglio, G. Totis, M. Sortino, and L. Fedrizzi, Corrosion behaviour of 316L stainless steel manufactured by selective laser melting, *Materials and Corrosion*, vol. 70, no. 9, pp. 1633–1645, 2019.
[10] European Hygienic Engineering Design Group, *EHEDG Guidelines Doc. 8: Hygienic Design Principles*, 3rd ed. 2018.
[11] J.-Y. Lee, A. P. Nagalingam, and S. H. Yeo, A review on the state-of-the-art of surface finishing processes and related ISO/ASTM standards for metal additive manufactured components, *Virtual and Physical Prototyping*, vol. 16, no. 1, pp. 68–96, 2021.
[12] Wohlers associates, Ed., *Post-Processing of AM and 3D-Printed Parts*. WOHLERS ASSOCIATES, 2021.
[13] R. Murcek, E. Fuchs, A. Boye, P. Joppa, and J. P. Majschak, Effect of structured surfaces on fouling and cleaning behaviour in plate heat exchangers, presented at the International Conference on Heat Exchanger Fouling and Cleaning, Enfield, Irland, 2015.
[14] M. Joppa, T. Hanisch, and M. Mauermann, Methodology for the assessment of cleanability and geometry optimization using flow simulation on the example of dimple-structured pipe surfaces, *Food and Bioproducts Processing*, vol. 132, pp. 141–154, 2022.
[15] T. Hanisch, M. Joppa, V. Eisenrauch, S. Jacob, and M. Mauermann, Optimizing the macrostructure of 3D-printed pipe surfaces to improve cleanability, *Heat Mass Transfer*, 2023.
[16] T. Hanisch, M. Joppa, V. Eisenrauch, S. Jacob, and M. Mauermann, Simulation-based optimization and experimental analysis of the cleanability of macro-structured, 3D-printed pipe surfaces with protrusions, *Food and Bioproducts Processing*, vol. 136, pp. 106–122, 2022.
[17] R. N. Oosterbeek, G. Sirbu, S. Hansal, K. Nai, and J. R. T. Jeffers, Effect of chemical–electrochemical surface treatment on the roughness and fatigue performance of porous titanium lattice structures, *Additive Manufacturing*, vol. 78, p. 103896, 2023.
[18] European Hygienic Engineering Design Group, *EHEDG Guidelines Doc. 2: A method for assessing the in-place cleanability of food processing equipment*, 3rd ed. 2007.
[19] M. Mauermann, J.-P. Majschak, T. Bley, C. Bellmann, A. Calvimontes, and A. Caspari, Cleanability of food contact surfaces with water jets, *Chemie Ingenieur Technik*, vol. 84, no. 9, pp. 1568–1574, 2012.
[20] A. Calvimontes, M. Mauermann, and C. Bellmann, Topographical Anisotropy and Wetting of Ground Stainless Steel Surfaces, *Materials*, vol. 5, no. 12, Art. no. 12, 2012.
[21] J. W. Tukey, Comparing Individual Means in the Analysis of Variance, *Biometrics*, vol. 5, no. 2, pp. 99–114, 1949.
[22] U. Bobe, Die Reinigbarkeit technischer Oberflächen im immergierten System, Technische Universität München, 2008. Accessed: 2024. [Online]. Available: https://mediatum.ub.tum.de/649731
[23] Sebastian Stelzer, METHOD FOR MANUFACTURING A COMPONENT WITH AN INTEGRATED CATHODE FOR AN ELECTROCHEMICAL POST-PROCESSING PROCESS AND FOR THE REMOVAL OF THE CATHODE FROM THE COMPONENT, WO23209080 A2, 2023

ISBN: 978-0-9984188-3-4; Published online www.heatexchanger-fouling.com